Solution Processing

Construction of Conjugated Carbon Nitride Nanoarchitectures in Solution at Low Temperatures for Photoredox Catalysis**

Yanjuan Cui, Zhengxin Ding, Xianzhi Fu, and Xinchen Wang*

Binary carbon nitrides (CNs) have attracted enormous attention owing to their versatile properties that allow prospective use as superhard materials, catalysts, semiconductors, and sensors.[1] Graphitic CN has the smallest band gap among various CN allotropes owing to the sp^2 hybridization of C and N atoms, forming a solid-state aromatic system that is inert against most acids and bases.[2] This cheap, easily available organic semiconductor was recently proposed as the basis for a new family of solar energy transducers, but also shows great promise in metal-free coordination chemistry, water splitting, heterogeneous organocatalysis, and environmental remediation.[3]

Covalent CN was first made by Berzelius, and the yellow "Pharaoh's serpent" thus formed was named in 1834 by Liebig as "melon".[4] The prediction in 1989 by Cohen and Liu that β-C_3N_4 was harder than diamond intensified research interests in CN chemistry.[5] A broad set of nitrogen-containing organics (e.g., cyanamide and melamine (MA)) have been employed to synthesize CN solids using bulk condensation routes, usually at 550°C.[6] This bulk condensation, however, suffers from kinetic problems. The introduction of the bulk reaction in a molten salt medium has been claimed to overcome this problem and to allow the production of crystalline graphitic CN.[7] High pressures and high temperatures were also applied to conquer the kinetic barriers. For example, CN solids have been synthesized by heating MA in hot hydrazine medium at 800°C and 3 GPa.[8] Wolf and coworkers obtained a graphitic derivative ($C_6N_9H_4Cl$) through a solid-state reaction of MA and cyanuric chloride (CC) at 1.5 GPa and 550°C.[9]

Soft solution-processing methods to assemble large polymeric superstructures at low temperature are especially attractive, because they enable rational bottom-up design of material structure by using molecular engineering, solution assembly, crystallization, and covalent cross-linking chemistry in a "one-pot" fashion. In the case of CN materials, low-temperature conditions are particularly indispensable, since

they can prevent nitrogen depletion from CN solids. But, the soft, low-temperature process requires catalysts. Montigaud et al. first obtained graphitic CN by the condensation of MA and CC using diisopropylethylamine as solvent and a base catalyst at 250°C and 130 MPa.[10] Modified solvothermal synthesis of a layered CN structure was subsequently reported by heating CC at 220–500°C in nonpolar organic solutions with $NaNH_2/NaN_3/Li_3N$ as nitriding agents and catalysts.[11] However, these reports focused on material synthesis and structure analysis only, lacking material function. Furthermore, the involvement of catalysts can passivate the surface of CNs.

It is therefore desirable to develop a catalyst-free, solution-assembly method to engineer the CN precursors into polymeric nanomaterials of a desired size and shape, particularly with 2D conjugated structures with minimized excitation binding energy that would allow the fast charge generation and separation, thus enabling their promising photochemical applications.[12]

Here, we first advanced the solution synthesis of CNs using CC and $NaNH_2$ with a pressurized hot or supercritical fluid technique that has been widely used for many chemical and material processes.[13] Besides temperature, the solvent in terms of viscosity, density, and polarity also plays a key role in the solution processing of soft matters.[14] Various hot solvents under autogenous pressure have therefore been examined as the reaction medium. Acetonitrile was found to facilitate CN synthesis, while the use of nonpolar solvents such as benzene; cyclohexane; or carbon tetrachloride restricted polymerization to tiny yields ($< 5\%$), although the expected conjugated CN network could be detected (Figure S1 and Table S1 in the Supporting Information). Obviously, more polar solvents promote the condensation and crystallization of CN moieties.

Since acetonitrile is an annealing fluid with a moderate critical temperature at 275°C and a low boiling point of 81°C, the use of this solvent also takes advantage of its unique properties as a subcritical fluid.[15] The substantial improved solubility and high diffusivity of the near-critical fluid in principle enhances mass transfer and accelerates the condensation kinetics. That way, it was possible to use hot acetonitrile for the condensation of CC and $NaNH_2$ to construct functional nanostructures of a supermolecular network of alternating C and N atoms; however those structures turned out to be photochemically inactive (Figure S2 in the Supporting Information), which is likely due to the incorporation of Na^+ ions as charge recombination centers, thus leading to catalyst poisoning.

Next, we employed the above optimized conditions, using MA instead of $NaNH_2$ as a monomer and an organic base to

[*] Y. Cui, Prof. Z. Ding, Prof. X. Fu, Prof. X. Wang
Research Institute of Photocatalysis, Fujian Provincial Laboratory of Photocatalysis-State Key Laboratory Breeding Base, and College of Chemistry and Chemical Engineering, Fuzhou University
Fuzhou 350002 (China)
E-mail: xcwang@fzu.edu.cn

facilitate the condensation process while excluding sodiumni-tride defects. That way, graphitic CN frameworks were produced from condensation of triazine tectons, such as CC and MA, in a subcritical acetonitrile at comparably low temperature by following the classic polymerization route as exemplified in Scheme 1.
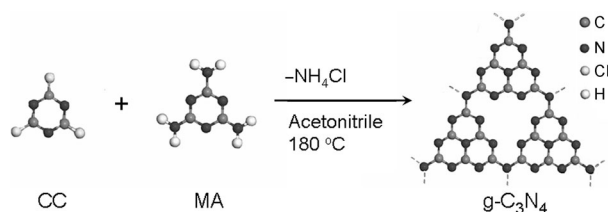
Scheme 1. Polymerization processes of cyanuric chloride (CC) and melamine (MA) in subcritical acetonitrile solvent.

The details of the catalyst-free synthesis are described in the experimental section in the Supporting Information. The resulting CN samples are denoted as LCN_{T-t}, where T refers to the solvothermal temperature (°C) and t is the condensation time (h). For comparison, graphitic CN (g-CN) was also synthesized by heating MA at 550 °C for four hours in air. The samples were applied as metal-free semiconductors for degradation of organic pollutants in water and also for photocatalytic H_2 evolution as illustrative model reactions quantifying the photochemical performance.

Compared to solid-state synthesis at high temperature, a significant feature of the hot-fluid technology is the comparably simple control of morphology. Samples composed of networks of primary nanobelts were obtained by polymerization of CC and MA in acetonitrile at 180 °C for 96 h (Figure 1a). From the overview image of the sample, it is
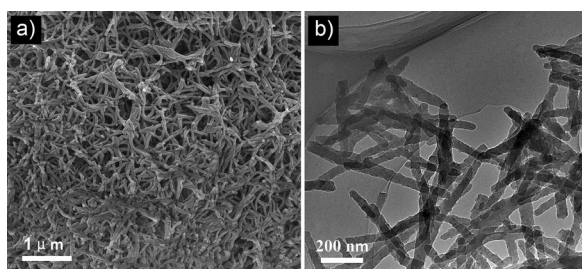

Figure 1. Typical a) SEM and b) TEM images of LCN_{180-96}, with the corresponding photograph in Figure S3 in the Supporting Information.

seen that the nanobelt content exceeds 90 % of the produced sample, with homogeneous widths of about 50–60 nm and lengths of the order of several micrometers. The typical TEM images (Figure 1b) show that the nanobelts are stable under the electron beam for a short period of time only, while exposure to the beam for extended time decomposes the structure and leads to an overall amorphization. When the synthesis temperature decreased from 180 to 160 and 140 °C, products with a less defined morphology were obtained (Figure S3 in the Supporting Information). When the samples

were kept at 180 °C but the annealing time was shortened to 48 and 24 h, anomalous nanorods were obtained. Clearly, hot-fluid annealing at certain conditions provides sufficient thermodynamic force to covalently link and assemble the molecular tectons to the hierarchical nanostructure.

XRD patterns (Figure S4a in the Supporting Information) of all samples that were synthesized by hot-fluid annealing at different temperatures present distinctive peaks at 27.4° ($d \approx 3.24$ Å), corresponding to the (002) interlayer reflection of a g-CN. But the peak intensities of samples constructed in solution are weaker than those of samples obtained by bulk polymerization at 550 °C. Moreover, the peaks at $2\theta \approx 13°$ (attributed to the in-planar repeated tri-*s*-triazine units) become broadened with increased reaction temperature and reaction time. At > 160 °C, the in-planar reflection peaks shift significantly from $2\theta \approx 13°$ to $2\theta \approx 11°$. These results indicated a regular in-planar connection of tri-*s*-triazine tectons in the CN layers, while some degree of disorder may exist in the packing of the CN layer. The evolution of undulation and "curls" during the assembly process in liquid medium may disturb the long-range packing of the CN layer along the (002) direction, as reflected already throughout the formation of nanobelt topology at 180 °C.

Fourier transformed infrared (FTIR) spectra (Figure S4b in the Supporting Information) of all products synthesized in the solution at different temperatures are characterized by a series of bands in the 1200–1700 cm⁻¹ region and a strong peak at approximately 800 cm⁻¹.[6,7] These IR bands are typical molecular vibration modes of triazine rings. The symmetric and antisymmetric -NH_2 stretching modes are found in the high-frequency region at approximately 3300 cm⁻¹. Notably, the absence of vibrations of -CH bonds near 3000 cm⁻¹ and -CN bonds near 2200 cm⁻¹ excludes the possibility of self trimerization of the -CN group in acetonitrile. This means that acetonitrile is not involved in the chemical reaction, but acts as a subcritical solvent to mediate the molecular solution assembly and the hierarchical construction.[16]

Carbon and nitrogen stoichiometry of the samples was determined by elemental analysis (Table 1). Results show that all products possess C/N molar ratios close to 0.77, slightly higher than the theoretical value of 0.75 for C_3N_4, that is, the material is slightly depleted in nitrogen.

N_2 sorption analysis revealed that the specific surface area of the as-synthesized LCN_{180-96} sample (30 m² g⁻¹) is approximately three times higher than that of g-CN. At elevated reaction temperature and prolonged reaction time the specific surface area of samples increased slightly, in agreement with the developed homogeneity in the nanostructural network.

Table 1: Physicochemical properties of LCN samples

Catalyst	Surface area [m² g⁻¹]	Molar ratio C/N	Band gap [eV]
g-CN	9	0.71	2.67
LCN_{140-48}	18	0.74	2.32
LCN_{160-48}	21	0.78	2.05
LCN_{180-48}	24	0.76	1.90
LCN_{180-24}	20	0.77	1.97
LCN_{180-96}	30	0.77	1.78

X-ray photoelectron spectroscopy (XPS) was used to measure the oxidation state of the prepared samples (Figure 2 a, b). High-resolution spectra of C1s at 286.25 eV and N1s at 398.82 eV are assigned to the sp^2 C=N bond in the *s*-triazine ring. The peaks at 288.45 eV and 284.6 eV in the C1s zone are attributed to electrons originating from an sp^2 C atom attached to a -NH$_2$ group and to an aromatic carbon atom.[6] The contribution at 399.95 and 400.55 eV in the N1s zone are ascribed to N atoms that are bound to three C atoms; these N atoms are located in the heptazine ring and as bridging atom, respectively.[6] These results support the assembly of CC and MA to the extended aromatic CN framework, which is largely based on heptazine repeating units.

The proposed heptazine structure in the CN framework was further confirmed by ^{13}C MAS NMR analysis (Figure 3). There are no resonances in the sp^3 region at $\delta = 0–70$ ppm and at 120 ppm. The spectrum of MA gives one peak at $\delta = 167.9$ ppm assigned to the presence of a C–NH$_2$ group; this spectrum is in good agreement with those reported by Damodaran et al.[17] The spectrum of CN$_{180-96}$ and g-CN samples shows two distinct peaks at $\delta = 164.5$ and 156.6 ppm. The first resonance is assigned to the C(e) atoms (CN$_2$(NH$_x$)), whereas the second one was attributed to the C(i) atoms of melem (CN3).[18] Different from MA, the chemical shifts assigned to C(e) of g-CN and CN$_{180-96}$ are shifted slightly to higher fields. This shift may result from the heptazine-based phases exhibiting a slightly higher degree of condensation.

The optical and electronic properties of LCNs were analyzed by UV/Vis diffuse reflectance spectroscopy (DRS) and electron paramagnetic resonance (EPR) technologies (Figure 2 c, d). Compared to a high-temperature bulk condensation method, the solvothermal processing in acetonitrile improves the π-electron delocalization in the conjugated system, thus the intrinsic optical and electronic properties of the resulting LCN polymers are greatly modified. Remarkably, the DRS spectra show a bathochromic shift of optical absorption from approximately 470 to 650 nm with increasing solvothermal temperature to 180 °C, as compared to bulk g-CN. Extended reaction times also promote the bathochromic shift in the optical absorption of samples, (Figure S5 in the Supporting Information). Clearly, the high mobility in the hot fluid improves the inter-planar packing towards J-type aggregates of heptazine building blocks, as reflected by the XRD analysis. The electronic band gap of a sample was determined from the Tauc plot, in which $(F(R)h\nu)^{\frac{1}{2}}$ (with $F(R) =$ diffuse absorption coefficient, $h =$ Planck constant, and $\nu =$ light frequency) is plotted versus the photon energy; the obtained band gaps are also listed in Table 1.

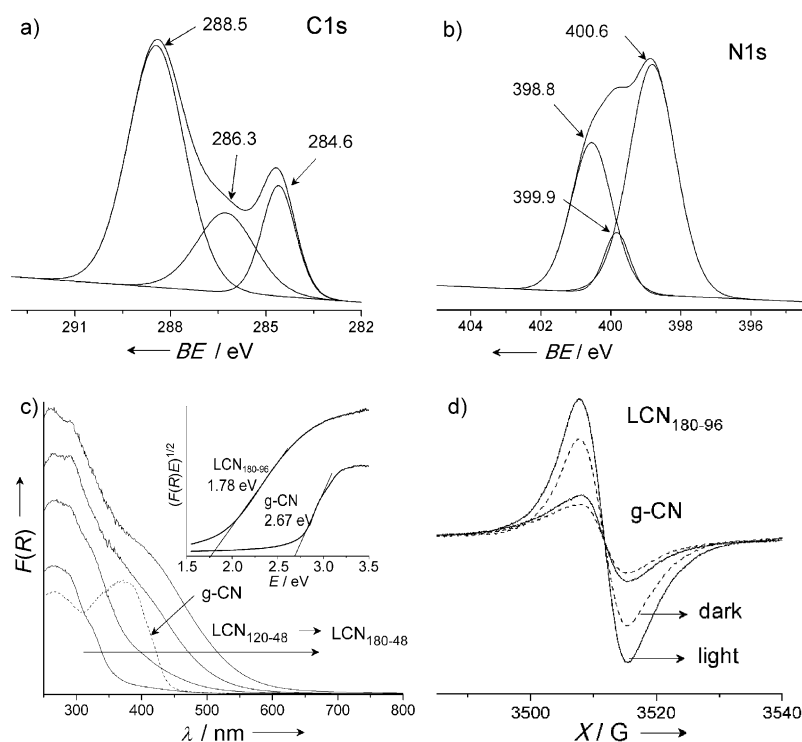The EPR spectrum of CN shows a slightly asymmetric signal line at a *g* value of 2.0032, indicating a small *g* aniso-

Figure 2. a, b) Core-level XPS spectra of C1s (a) and N1s (b) of LCN$_{180-96}$ (*BE* = binding energy); c) UV/Vis diffuse reflectance spectra of LCN$_{T-48}$. The inset shows the bandgap determination of g-CN and LCN$_{180-96}$ form the Tauc plots. d) Solid-state ESR spectra of LCN$_{180-96}$ and g-CN with visible light or in the dark (*X* = magnetic field strength).
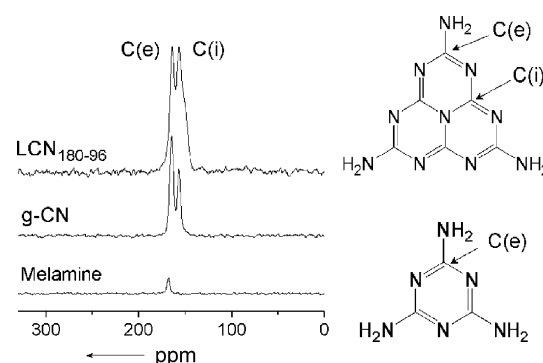
Figure 3. ^{13}C MAS NMR spectra for melamine, g-CN, and LCN$_{180-96}$.

tropy with an estimated uniform electron species (Figure S6 in the Supporting Information). It is well-known that $g = 2.0032$ is attributed to an unpaired electron on carbon atoms of the aromatic rings within p-bonded nanosized clusters.[19] The intensity of signals for LCN samples gradually increases with the increase in the reaction time and temperature, thus indicating the progressive development of electronic band structure. Upon irradiation, the EPR signals of LCN$_{180-96}$ are greatly enhanced. This is a strong indication that the efficient generation of photochemical radical pairs occurred in the solvothermal CN polymers. Note that when the reaction temperature is lower than 160 °C, the signal

intensity is considerably weakened. It again shows that sufficient thermal energy is crucial for the structural reshuffling of C and N atoms towards a more conjugated, more stable structure.

Mott–Schottky analysis (Figure S7 in the Supporting Information) of LCN_{180-96} was carried out and the typical plot suggests n-type characteristic of LCN_{180-96}.[12a] The flat-band potential is estimated to be at -1.26 V versus Ag/AgCl, and the position of the valence band at 0.52 eV.

The photocatalytic performance of LCN samples for water treatment with visible light was evaluated by degradation of organic pollutants, including the model dye Rhodamine B (RhB), *p*-chlorophenol (4-CP), and phenol. After light illumination for one hour ($\lambda > 420$ nm), more than 95% of RhB was bleached by LCN_{180-96}, and the durability of catalyst was well-kept after five repeated runs (Figure S8 in the Supporting Information). Moreover, LCN showed a high photocatalytic activity towards hydroxylated aromatic compounds like 4-CP and phenol. The LCN samples gave a significantly improved degradation rate compared to g-CN (Figure 4). Synthetic conditions dramatically influence the reactivity of LCN solids for the degradation of both 4-CP and phenol, and it was found that LCN_{180-96} has the highest reactivity. After three hours reaction, about 95% 4-CP and 91% phenol were degraded by light-excited LCN_{180-96}. A 15 h recycling experiment showed that LCN_{180-96} is a stable photocatalyst (Figure S8 in the Supporting Information). The enhanced photocatalytic activity of LCN could be ascribed to the formation of a complex nanostructure promoting charge separation at the interface.

The photochemical performance of LCN samples was further illustrated by light-induced H_2 evolution from protic solution. Only a trace amount of H_2 was detected for LCN_{160-48} and LCN_{140-48}, accompanied by a production of N_2 (Figure 4b). When the synthesis temperature was increased to 180 °C, the H_2 evolution rate (HER) was enhanced to 2.8, 4.9, and 6.1 μmol h^{-1} for LCN_{180-24}, LCN_{180-48}, and LCN_{180-96}, respectively. Moreover, the amount of produced H_2 increased synchronously as a function of irradiation time. These findings can be interpreted by the fact that the higher temperature and longer reaction time of the hot fluid annealing promote the condensation of CN, favoring surface kinetics of photocatalysis. Nevertheless, when the reaction temperature was increased to 230 °C, the LCN_{230-48} sample showed a dramatically decrease in the HER (1.6 μmol h^{-1}), which is likely due to the solvothermally induced carbonization of LCN_{230-48} (the sample is black). Such a carbonization has already observed for the hydrothermally induced formation of nanostructured carbon from N-containing biomasses.[20] Note that g-CN synthesized by the bulk condensation at 530 °C can catalyze H_2 evolution at a comparable rate of 4.7 μmol h^{-1} to that of LCN_{180} samples (Table S2 in the Supporting Information). It is however a remarkable observation that CN synthesized at such a low temperature of 180 °C can achieve photoredox catalysis, thus again underlining the positive role of hot acetonitrile fluid on supporting CN synthesis.

In conclusion, a catalyst-free, solution-processed approach has been developed for the textural engineering of triazine monomers to CN nanomaterials. The as-obtained superstructure possesses a decreased band gap and enhanced light-harvesting capability. The photocatalytic activity of the LCN samples for organic pollutant degradation was greatly improved over the traditional g-CN samples. The H_2 evolution activity of LCN samples was comparative to that of g-CN; however the considerable low synthesis temperature without employment of extra catalysts was a breakthrough in CN chemistry. We believe that this innovative assembly route in solution for nanostructured CN at mild conditions will offer a new avenue to construct CN-based semiconductors by integrating this route to diverse approaches for modification in solution at low temperatures. That way, chemical composition, electronic structure, and surface functionality can be much better engineered for advanced applications in the fields of catalysis, energy, and environmental remediation.
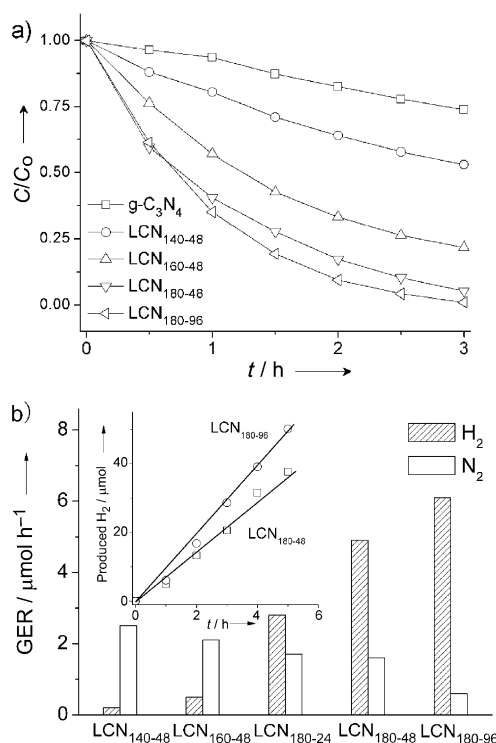
Figure 4. Photocatalytic activity of LCN samples under illumination with visible light: a) degradation of 4-CP; b) evolution of H_2. The inset in (b) shows the H_2 evolution from protic solution as a function of reaction time. GER in (b) stands for gas evolution rate of H_2 or N_2.

[1] a) D. M. Teter, R. J. Hemley, *Science* **1996**, *271*, 53; b) R. B. Kaner, J. J. Gilman, S. H. Tolbert, *Science* **2005**, *308*, 1268; c) E. Kroke, M. Schwarz, *Coord. Chem. Rev.* **2004**, *248*, 493; d) Y. J. Zhang, M. Antonietti, *Chem. Asian J.* **2010**, *5*, 1307; e) J. S. Lee, X. Q. Wang, H. M. Luo, G. A. Baker, S. Dai, *J. Am. Chem. Soc.* **2009**, *131*, 4596; f) J. S. Lee, X. Q. Wang, H. M. Luo, S. Dai, *Adv. Mater.* **2010**, *22*, 1004.

[2] X. C. Wang, X. F. Chen, A. Thomas, X. Z. Fu, M. Antonietti, *Adv. Mater.* **2009**, *21*, 1609.

[3] a) X. C. Wang, K. Maeda, A. Thomas, K. Takanabe, G. Xin, J. M. Carlsson, K. Domen, M. Antonietti, *Nat. Mater.* **2009**, *8*, 76; b) J. S. Zhang, M. Grzelczak, Y. D. Hou, K. Maeda, K. Domen, X. Z. Fu, M. Antonietti, X. C. Wang, *Chem. Sci.* **2012**, *3*, 443; c) X. Zhu, C. C. Tian, S. M. Mahurin, S. H. Chai, C. M. Wang, S. S. Brown, G. M. Veith, H. M. Luo, H. L. Liu, S. Dai, *J. Am. Chem. Soc.* **2012**, *134*, 10478; d) Y. J. Cui, J. H. Huang, X. Z. Fu, X. C. Wang, *Catal. Sci. Technol.* **2012**, *2*, 1396.

[4] J. V. Liebig, *Ann. Pharm.* **1834**, *10*, 10.

[5] A. Y. Liu, M. L. Cohen, *Science* **1989**, *245*, 841.

[6] A. Thomas, A. Fischer, F. Goettmann, M. Antonietti, J. Müller, R. Schlögl, J. M. Carlsson, *J. Mater. Chem.* **2008**, *18*, 4893.

[7] M. J. Bojdys, J. Müller, M. Antonietti, A. Thomas, *Chem. Eur. J.* **2008**, *14*, 8177.

[8] a) H. Montigaud, B. Tanguy, G. Demazeau, I. Alves, M. Birot, J. Dunogues, *Diamond Relat. Mater.* **1999**, *8*, 1707; b) G. Demazeau, *J. Mater. Chem.* **1999**, *9*, 15; c) L. Alves, G. Demazeau, B. Tanguy, F. Weill, *Solid State Commun.* **1999**, *109*, 697.

[9] Z. H. Zhang, K. Leinenweber, M. Bauer, L. A. J. Garvie, P. F. McMillan, G. H. Wolf, *J. Am. Chem. Soc.* **2001**, *123*, 7788.

[10] H. Montigaud, B. Tanguy, G. Demazeau, S. Courjault, M. J. Birot, J. Dunogues, *C. R. Acad. Sci. Ser. IIb* **1997**, *325*, 229.

[11] a) V. N. Khabashesku, J. L. Zimmerman, J. L. Margrave, *Chem. Mater.* **2000**, *12*, 3264; b) J. L. Zimmerman, R. Williams, V. N. Khabashesku, J. L. Margrave, *Nano Lett.* **2001**, *1*, 731; c) Q. X. Guo, Y. Xie, X. J. Wang, S. Y. Zhang, T. Hou, S. C. Lv, *Chem. Commun.* **2004**, 26; d) Q. X. Guo, Q. Yang, C. Q. Yi, L. Zhu, Y. Xie, *Carbon* **2005**, *43*, 1386; e) Q. Fu, C. B. Cao, H. S. Zhu, *Chem. Phys. Lett.* **1999**, *314*, 223; f) Q. X. Guo, Y. Xie, X. J. Wang, S. C. Lv, T. Hou, X. M. Liu, *Chem. Phys. Lett.* **2003**, *380*, 84.

[12] a) J. S. Zhang, X. F. Chen, K. Takanabe, K. Maeda, K. Domen, J. D. Epping, X. Z. Fu, M. Antonietti, X. C. Wang, *Angew. Chem.* **2010**, *122*, 451; *Angew. Chem. Int. Ed.* **2010**, *49*, 441; b) X. F. Chen, Y. S. Jun, K. Takanabe, K. Maeda, K. Domen, X. Z. Fu, M. Antonietti, X. C. Wang, *Chem. Mater.* **2009**, *21*, 4093; c) X. C. Wang, K. Maeda, X. F. Chen, K. Takanabe, K. Domen, Y. D. Hou, X. Z. Fu, M. Antonietti, *J. Am. Chem. Soc.* **2009**, *131*, 1680; d) J. S. Zhang, M. W. Zhang, R. Q. Sun, X. C. Wang, *Angew. Chem.* **2012**, *124*, 10292; *Angew. Chem. Int. Ed.* **2012**, *51*, 10145; e) F. Z. Su, S. C. Mathew, L. Möhlmann, M. Antonietti, X. C. Wang, S. Blechert, *Angew. Chem.* **2011**, *123*, 683; *Angew. Chem. Int. Ed.* **2011**, *50*, 657; f) J. H. Sun, J. S. Zhang, M. W. Zhang, M. Antonietti, X. Z. Fu, X. C. Wang, *Nat. Commun.* **2012**, DOI:10.1038/ncomms2152.

[13] a) A. R. Katritzky, D. A. Nichols, M. Siskin, R. Murugan, M. Balasubramanian, *Chem. Rev.* **2001**, *101*, 837; b) A. Baiker, *Chem. Rev.* **1999**, *99*, 453; c) P. E. Savage, S. Gopalan, T. I. Mizan, C. J. Martino, E. E. Brock, *AIChE J.* **1995**, *41*, 1723.

[14] a) Y. P. Sun, M. A. Fox, K. P. Johnston, *J. Am. Chem. Soc.* **1992**, *114*, 1187; b) C. F. Weber, R. Puchta, N. J. R. Van Eikema Hommes, P. Wasserscheid, R. Van Eldik, *Angew. Chem.* **2005**, *117*, 6187; *Angew. Chem. Int. Ed.* **2005**, *44*, 6033.

[15] a) J. D. Martin, R. F. Hess, P. D. Boyle, *Inorg. Chem.* **2004**, *43*, 3242; b) J. P. Zhang, Y. Y. Lin, X. C. Huang, X. M. Chen, *J. Am. Chem. Soc.* **2005**, *127*, 5495.

[16] a) M. X. Li, H. Wang, S. W. Liang, M. Shao, X. He, Z. X. Wang, *Cryst. Growth Des.* **2009**, *9*, 4626; b) W. Qian, R. Hao, Y. L. Hou, Y. Tian, C. M. Shen, H. J. Gao, X. L. Liang, *Nano Res.* **2009**, *2*, 706.

[17] K. Damodaran, G. J. Sanjayan, P. R. Rajamohanan, S. Ganapathy, K. N. Ganesh, *Org. Lett.* **2001**, *3*, 1921.

[18] B. Jürgens, E. Irran, J. Senker, P. Kroll, H. Müller, W. Schnick, *J. Am. Chem. Soc.* **2003**, *125*, 10288.

[19] a) M. Tabbal, T. Christidis, S. Isber, P. Merel, M. A. E. Khakani, M. Chaker, A. Amassian, L. Martinu, *J. Appl. Phys.* **2005**, *98*, 044310; b) J. S. Zhang, G. G. Zhang, X. F. Chen, S. Lin, L. Möhlmann, G. Dolega, G. Lipner, M. Antonietti, S. Blechert, X. C. Wang, *Angew. Chem.* **2012**, *124*, 3237; *Angew. Chem. Int. Ed.* **2012**, *51*, 3183.

[20] L. Zhao, L. Z. Fan, M. Q. Zhou, H. Guan, S. Y. Qiao, M. Antonietti, M. M. Titirici, *Adv. Mater.* **2010**, *22*, 5202.